Proceedings of ASME Turbo Expo 2019:
Turbomachinery Technical Conference and Exposition
GT2019
June 17-21, 2019, Phoenix, Arizona, USA

GT2019-91437

MULTIPHYSICS NUMERICAL INVESTIGATION OF AN AERONAUTICAL LEAN BURN COMBUSTOR

D. Bertini*, L. Mazzei, A. Andreini, B. Facchini
Department of Industrial Engineering
University of Florence
50139, via S. Marta 3, Florence, Italy
Tel: +39 055 275 8771
davide.bertini@htc.unifi.it

ABSTRACT

The importance of the combustion chamber has been underestimated for years by aeroengine manufacturers that focused their research efforts mainly on other components, such as compressor and turbine, to improve the engine performance. Nevertheless, stricter requirements on pollutant emissions have contributed to increase the interest on combustor development and, nowadays, new design concepts are widely investigated. To meet the goals of ACARE FlightPath 2050 and future ICAO-CAEP standards one of the most promising results is provided by the Lean Burn technology. As this combustion mode is based on a lean Primary Zone, the air devoted to liner cooling is restricted and advanced cooling systems must be exploited to obtain higher overall effectiveness. The pushing trends of Turbine Inlet Temperature and Overall Pressure Ratio in modern aeroengine are not supported enough by the development of materials, thus making the research branch of liner cooling increasingly relevant.

In this context, Computational Fluid Dynamics is able to predict the flow field and the complex interactions between the involved phenomena, supporting the design of modern Lean Burn combustors in all stages of the process. RANS approaches provide a solution of the problem with low computational cost, but can lack in accuracy when the flow unsteadiness dominates the fluid dynamics and the strong interactions, as in aeroengine combustors. Even if steady simulations can be easily employed in the preliminary design, their inaccuracy can be detrimental for an optimized combustor design and Scale-Resolving methods should be preferred, at least, in the final stages. Unfortunately, having to deal with a multiphysics problem as Conjugate Heat Transfer (CHT) in presence of radiation, these simulations can become computationally expensive and some numerical treatments are required to handle the wide range of time and space scales in an unsteady framework.

In the present work the metal temperature distribution is investigated from a numerical perspective on a full annular aeronautical lean burn combustor operated at real conditions. For this purpose, the U-THERM3D multiphysics tool was developed in ANSYS Fluent and applied on the test case. The results are compared against RANS and experimental data to assess the tool capability to handle the CHT problem in the context of scale-resolving simulations.

NOMENCLATURE

B_M	Mass Spalding number	$[-]$
c	Progress variable	$[-]$
d	Droplet diameter	$[m]$
D	Mass diffusivity	$[m^2\ s^{-1}]$
L	Length scale	$[m]$
P	Pressure	$[Pa]$
P/T	Pilot-to-total fuel split	$[\%]$

*Corresponding author

q''	Heat flux	$[W\ m^{-2}]$
S_r	Source of radiative energy	$[W\ m^{-3}]$
S_h	Sherwood number	$[-]$
T	Temperature	$[K]$
We	Weber number	$[-]$
s	Curvilinear abscissa	$[m]$
Y	Species mass fraction	$[-]$
Z	Mixture fraction	$[-]$

Acronyms

ACARE	Advisory Council for Aeronautics Research in Europe
BC	Boundary Condition
CAEP	Committee on Aviation Environmental Protection
CFD	Computational Fluid Dynamics
CHT	Conjugate Heat Transfer
CIAM	Central Institute of Aviation Motors
DES	Detached Eddy Simulation
DO	Discrete Ordinate
FAR	Fuel Air Ratio
FGM	Flamelet Generated Manifold
ICAO	International Civil Aviation Organization
LES	Large Eddy Simulation
NSE	Navier Stokes Equation
NEWAC	NEW Aero engine core Concepts
OPR	Overall Pressure Ratio
PDF	Probability Density Function
PERM	Partial Evaporation and Rapid Mixing
RANS	Reynolds Averaged Navier Stokes
RTE	Radiative Transfer Equation
SAFE	Source bAsed eFfusion modEl
SAS	Scale Adaptive Simulation
SRS	Scale-Resolving Simulation
TIT	Turbine Inlet Temperature
UDF	User Defined Function

Greek

ω	Turbulence frequency	$[s^{-1}]$
Θ	Spanwise angle	$[^\circ]$
ψ	Generic variable	$[-]$
ρ	Density	$[kg\ m^{-3}]$

Subscripts

40	Referred to Plane 40 (combustor exit)
c	Progress variable
eq	Equilibrium
g	Gas phase
rad	Radiation
vK	von Karman
w	Wall

INTRODUCTION

Aviation is increasingly gaining a key role in mid-long range transportation of people. The improvement in safety and the cost reduction of air travel have lead to the growth of passenger demand over the past 20 years and this trend will continue in the next future. Recent ICAO forecasts [1] estimated an average growth per year of about 4.0% in air traffic for the 2020-2040 period.

In last years, the people sensibility to environmental issues is deeply affecting the aeroengine industry that has to face the pressing demands for engines with lower pollutant emissions, as established firstly by ICAO-CAEP/6 for NOx (-60%) and then by ICAO-CAEP/10 for CO_2 and nvPM. Moreover, the evolving technology and international scenario have recently called into question the sufficiency of existing goals of ACARE Vision 2020 that, for this reason, were revised and their horizon was extended towards 2050 with the Flightpath 2050 to further break down NO_x and CO_2.

In this context, great research effort is devoted to improve performance of the engine, mainly increasing Turbine Inlet Temperature (TIT) and Overall Pressure Ratio (OPR). However, all the hot path components, that are the combustor and turbine, undergo stronger thermal stresses that could lead to dangerous engine damages and failures. Focusing on the combustor, aforementioned improvements lead to higher coolant and flame temperature. The former reduces the cooling potential, while the latter increases the thermal load on the hot side. As a result, the control of liner temperature becomes more challenging.

Independently by the combustor architecture, the cooling system can be strongly stressed. Indeed, the requirements for control of exit gas temperature, emissions and metal temperature generate an intense competition for the utilization of combustor airflow [2]. The flow split is mainly chosen according to design requirements about profile temperature as well as pollutant emissions. The residual excess air is demanded to keep liner temperature below a critical value and avoid high metal temperature gradients. Unfortunately, the achievement of low NO_x emissions is in contrast with the future trends of TIT and OPR. The technology challenge of these last decades regarding the emission abatement on aeroengines for civil market is leading to deep modifications in the concept design of aeroengine combustors. The standard RQL technology has almost approached an asymptote in terms of reduction in pollutant emissions and will be unable to respect the future limits for NO_x, CO and soot. To meet the stringent regulations some engine manufactures have focused the research efforts on Lean Direct Injection (LDI) technology, where almost all the effluent compressor air (i.e. about 70% of the total inflow) is delivered to the primary zone in order to have a lean homogeneous mixture and, then, lower temperature peaks [3]. In these conditions, the cooling system could lack of coolant and to avoid an overheating of the liner highly-effective cooling strategies are required. Literature on combus-

tor cooling is rich in technical solutions, such as effusion cooling, double-wall configurations, thermal barrier coating, matrix cooling and traspiration cooling [4]. In particular, during past years, multi-perforated liners have gained a key role thanks to its double benefit: film coverage that protects the liner from hot gases and heat sink within holes due to the passage of coolant [5]. This technique is the object of many experimental and numerical studies focused on the configuration of the multi-perforation [5–8] as well as on the interaction between swirling flow and film coverage [9–15].

Considering the cost and the difficulties related to experimental campaigns at high pressure and temperature conditions, Computational Fluid Dynamics (CFD) has been adopted as primary tool to have a deeper insight into the involved phenomena of modern aeroengine combustors. Nevertheless, the complex interaction between turbulence, combustion, radiation and heat conduction makes the prediction of metal temperatures challenging and multiphysics methods are required. RANS approaches, i.e. the standard tool in industrial framework, are useful for the preliminary design but they are not always suitable as high-fidelity tool. Indeed, in swirling reacting flows turbulence has huge effects on both the chemistry and spray as well as on the wall heat fluxes. For this reason, the aerothermal field cannot be properly predicted by RANS and Scale-Resolving Simulations (SRSs) should be recommended [16–18]. However, the unsteady nature of SRSs requires to handle a wide range of time scales involved in Conjugate Heat Transfer (CHT) problems. The long response time of solid makes fully-coupled methods infeasible in an unsteady framework. On the other hand, in order to effectively overcome this issue and minimize the CPU cost, loose coupling is preferred where different simulations are devoted to each physics exchanging only some quantities at a given frequency at the interface between two coupled domains. Several approaches can be found in literature, suitable for the prediction of long transient [19, 20] or quasi-steady [21–23] metal temperature.

The objective of the present work is the development and assessment of a multiphysics tool, named U-THERM3D, for high-fidelity predictions of metal temperature using the code ANSYS Fluent in the context of Scale Resolving Simulations. For this purpose, the full-annular combustor developed by Avio Aero in the framework of the LEMCOTEC project and equipped with the PERM injection system (Partially Evaporated and Rapid Mixing) is considered. The experimental measurements performed at the Central Institute of Aviation Motors (CIAM) on such combustor allowed to obtain valuable data at several operating conditions both in terms of pollutant emissions, wall temperature and exit temperature profile. On the same annular combustor steady analyses with the THERM3D tool were performed in [24] to predict metal temperature, whereas SRSs were adopted in [25] for an accurate characterization of aerothermal field in the flametube, with focus on profile temperature at exit and pollutant emissions. The results have revealed that Conjugate Heat Transfer can take advantage of a scale-resolving treatment of turbulence and this work tries to be the missed link between [24] and [25]. To the authors' knowledge no works can be found in literature on multiphysics simulations of lean burn combustors relying on Scale Adaptive Simulation. For this reason, the present work aims to be a reference for high-fidelity final design and a starting point for future activities as well.

The paper is structured as follows: the first part is devoted to the description of the experimental test case. Then, the U-THERM3D procedure will be explained together with the main mathematical models used to address the physical phenomena involved in a reactive two-phase flow. In the second part, results obtained at Approach and Take-Off operations will be shown and the main heat transfer modes of such a real aeroengine combustor will be investigated.

EXPERIMENTAL TEST CASE

LEMCOTEC combustor

The present work investigates a single annular combustor designed in the EU-funded research program LEMCOTEC. The fluid dynamics behavior is characterized by air passing through a dump diffuser and diverted within the cowl and to the inner/outer annuli, where it cools the liner and is partly bled outside. Once inside the cowl, it flows through the swirler and the dome cooling system. An impingement-cooled heat shield protects the dome, which provides also slot cooling in the first part of the liner. Such liners are cooled also by staggered effusion holes. The prototype can be considered an improvement of the combustor designed, manufactured and tested in a previous research program (NEWAC) and depicted in Figure 1. For the sake of brevity and confidentiality, we can mention only that such an improvement concerns the volume and the shape of the flametube but also the effusion cooling system, so as to reduce emissions and enhance the durability of the liners. Another significant modification consisted in the use of a different injection system and the redefinition of the combustor flow split.

FIGURE 1. Avio Aero's NEWAC combustor.

The lean burn concept was exploited in the test article to achieve low NO_x emission. The injection system is the so-called PERM (Partial Evaporation and Rapid Mixing), designed to operate at medium OPR ($20 < OPR < 35$). As sketched in Figure 2 the device is characterized by co-rotating double radial swirlers. Fuel staging is exploited between a pressure atomizer (pilot injection for low power stability) and an air blast that forms a liquid film on the outer side of the lip (main injection for low emissions at high power).

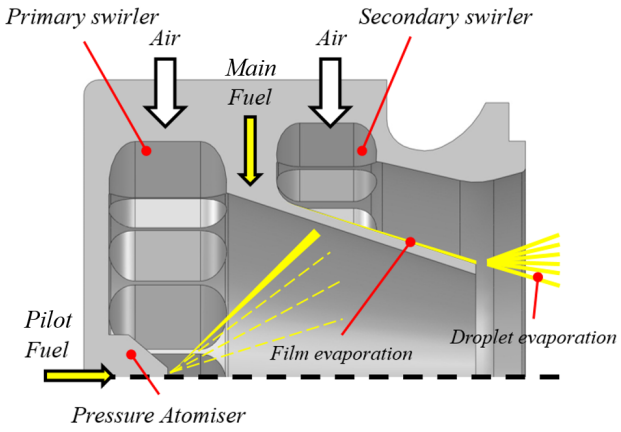

FIGURE 2. Sketch of the PERM injection system equipped on the LEMCOTEC combustor.

The validation of the design process was carried out at the end of the project through full annular reactive tests at the Central Institute of Aviation Motors (CIAM). Several operating points were investigated at CIAM, nevertheless only Approach and Take-Off were chosen in this activity and the data collected during the experimental campaign are reported in the present paper. Table 1 reports the details of the operating conditions considered in this work.

TABLE 1. Description of the investigated test points. Underlined the value of P/T used in the CFD simulations.

Test point	P30	T30	FAR	P/T	Active
	bar	K	‰	%	injectors
Approach (ICAO 30)	13.5	655	17.2	70	18
Take-Off (ICAO 100)	19.0	840	28.3	10	18

During the experimental campaign metal temperature measurements were collected with thermocouples equipped on the cold side of the liners. Measurement points were located in selected sectors at different angular positions and grouped to obtain a tangential distribution for a single ideal sector. A traverse system was used at the combustor exit to sample the gas emissions and analyse the temperature pattern (see Figure 3), which however are not the objective of this work and were better discussed in a previous work focused on the prediction of the aerothermal field with Scale-Adaptive Simulation (SAS) [25].

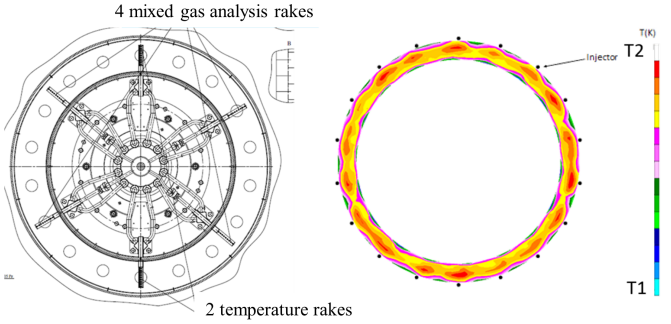

FIGURE 3. Sketch of the traverse system (left) and example of resulting temperature pattern for the Approach condition (right).

NUMERICAL DETAILS

The commercial code ANSYS Fluent Release 17.1 was used to carry out all the simulations here reported.

Turbulence Modelling

The SAS-SST model was used to solve the compressible Navier Stokes Equations (NSEs) for the reacting mixture. This approach consists in a Unsteady Reynolds Averaged Navier Stokes (URANS) formulation exploiting the von Karman length scale L_{vK} into the ω-equation as source term Q_{SAS} to increase the dissipation and reduce the local eddy viscosity [26]:

$$Q_{SAS} = max\left[\rho\zeta_2\kappa S^2\left(\frac{L}{L_{vK}}\right)^2 - C\frac{2\rho k}{\sigma_\phi}max\left(\frac{|\nabla\omega|}{\omega^2},\frac{|\nabla k|}{k^2}\right),0\right] \quad (1)$$

where ζ_2, σ_ϕ and C are model constant, κ is the von Karman constant and S is the strain rate tensor. In Equation 1 L represents the integral turbulent length scale computed by the modelled turbulence as in RANS whereas L_{vK} is defined as:

$$L_{vK} = \kappa\left|\frac{U'}{U''}\right| \quad (2)$$

and depends on the first and second derivatives of the velocity field as:

$$|U'| = \sqrt{\frac{\partial U_i}{\partial x_j}\frac{\partial U_i}{\partial x_j}}; \quad |U''| = \sqrt{\frac{\partial^2 U_i}{\partial x_j^2}\frac{\partial^2 U_i}{\partial x_k^2}}; \tag{3}$$

The SAS model represents a robust choice, as preserves a RANS mode in flow fields with reduced instability, while it provides LES-like results for very unsteady flows such as swirling jets. This feature is useful to save computational resources in confined flows because closer to wall the model works as a RANS simulation limiting the mesh constraints typical of LES approaches and the sudden rise of grid elements. The robustness of this approach is also ensured by the prevention of typical issues related to Detached Eddy Simulation (DES) models, such as grid-induced separation as well as the strong sensitivity to mesh size. Indeed, the present model adjusts the turbulence length scale depending on the local flow inhomogeneities through the scale L_{vK}. Unlike LES, however, SAS is not formulated to be based on the grid size for the scale resolution but the break-up of large eddies into a turbulent spectrum is driven by L_{vK} and then dynamically adjust. Nevertheless, adequate spatial and temporal discretizations have to be used to correctly solve the small scales in zones where an LES solution is required, avoiding unphysical damping in the energy cascade process and the overprediction of turbulent viscosity which could be detrimental to obtain an unsteady fluctuating solution.

Combustion Modelling

The Flamelet Generated Manifold (FGM) combustion model was chosen to reproduce the features of the lean spray flame as proved by previous works [17, 18]. According to this approach, a solution of a set of laminar adiabatic one-dimensional flamelets generates a two-dimensional manifold $\phi(Z,c)$, accounting for the non-adiabatic effects with an enthalpy defect approach [27]. Two key variables are used to parametrize the chemical state of the flamelets, i.e. the mixture fraction Z and the normalized progress variable $c = Y_c/Y_{c,eq}$. The definition of the transition from fresh to burnt gases, provided by the unnormalized reaction progress variable, was chosen as $Y_c = Y_{CO} + Y_{CO_2}$. The manifold was generated using a set of 64x64 non-premixed flamelets. The effects of turbulence-chemistry interaction were included integrating the laminar quantities of the manifold in a pre-processing step using a presumed β-Probability Density Function (β-PDF) for both mixture fraction and progress variable, as in [28]. Considering a laminar quantity $\psi(c,Z)$ and assuming Z and c are statistically independent in the flame, the integrated value was obtained as:

$$\tilde{\psi} = \int\int \psi(c,Z) PDF(c,\tilde{c},\widetilde{c''^2}) PDF(Z,\tilde{Z},\widetilde{Z''^2})\,\mathrm{d}c\mathrm{d}Z \tag{4}$$

where $\tilde{c}$, $\tilde{Z}$ and $\widetilde{c''^2}$, $\widetilde{Z''^2}$ are respectively the mean values and variances of progress variable and mixture fraction.

Four additional transport equations were solved to obtain the scalar fields of these quantities. The source terms for mixture fraction and progress variable accounts respectively for liquid fuel evaporation and chemical reaction effects. The turbulent $\tilde{c}$-source term is modelled using a finite rate assumption, integrating its laminar value by means of Eq. 4. The simulations reported in the present work were performed modelling kerosene as pure $C_{10}H_{22}$ (n-decane), using a detailed reaction mechanism taken from [29] with 96 species and 856 reactions.

Spray Modelling

The presence of liquid fuel was modelled using a coupled Lagrangian-Eulerian formulation, neglecting the primary breakup process ascribable to the atomization of the liquid film. The phenomena occurring in the dense spray region were modelled injecting a diluted spray whose droplets are subject to motion, heat transfer, evaporation and secondary breakup. The two-way coupling with the gas phase was accounted for by considering such phenomena. Drag effects for the liquid momentum equations were computed assuming the drag coefficients of a spherical non-deformable droplet [30]. The WAVE model [31] was chosen for secondary breakup due to the high Weber number (i.e. We >100). Turbulent fluctuating components of particle velocity were neglected since the SAS model directly resolves the most energy-carrying vortices. Evaporation was modelled with a uniform temperature approach [32], assuming that the process is mainly governed by the gradient of fuel vapour concentration at the droplet surface, a widely accepted hypothesis for dilute sprays. The fuel vapour is considered in equilibrium with the liquid, thus the vapour partial pressure is equal to the saturation value at the droplet temperature. This implies that the flux of fuel vapour in the carrier phase is related to the difference in vapour concentration at the droplet surface and in the bulk gas, leading to the following expression for the evaporation rate:

$$\tilde{\dot{m}}_d = -\pi d \rho D S_h B_M \tag{5}$$

where d is the droplet diameter, ρ and D are density and mass diffusivity of the air-vapour mixture and B_M represents the mass Spalding number [32]. S_h expresses the Sherwood number, evaluated as a function of Schmidt and particle Reynolds numbers [33]. The technical report published by [34] was used to characterize Jet A-1 fuel.

Radiation modelling

The radiation between burnt gas mixture and metal, in addition to the gas-gas and solid-solid radiative interactions, are computed by the Radiative Transfer Equation (RTE). Considering a polar coordinate system the Discrete Ordinate (DO) model [35] is a ray tracing approach to solve the RTE for a discrete number of $N_\theta \times N_\phi$ solid angles representing the beam directions. The radiative balance is applied in the control volumes for each direction. As the RTEs, i.e. one for each direction, are projected and solved into the Cartesian coordinate system the same numerical treatments of NSEs are used to solve the radiation problem. Such a discretization can lead to a misalignment between solid angle directions and face normals of the control volume. This overhang causes inaccuracy in the computation of fluxes of radiation intensity. To correctly account for the overhanging fraction a pixelation is applied to the overhang angles, dividing the solid angle in $N_{\theta_p} \times N_{\phi_p}$ pixels.

In the present work, a 4x4 angular discretization and 3x3 pixelation were set to limit the huge computational effort of the DO model. A validation of the radiation modelling approach can be found in [36].

U-THERM3D

In order to solve a multiphysics CHT problem in an unsteady fashion, a coupling code was developed in ANSYS Fluent framework. In the past years, a 3D coupled approach for the thermal design of combustor liners, called THERM3D, was developed by Mazzei [37] in ANSYS CFX for steady applications and extended to ANSYS Fluent in [24]. Such a tool, however, is limited in its applicability to RANS approaches because of the steady-based formulation of the solution algorithm and the new tool (i.e. U-THERM3D) aims to fulfill the need of a loosely coupled algorithm for SRSs.

The basic idea behind U-THERM3D procedure is a desynchronisation of time steps in the solution of the involved phenomena, that can be summarized in convection (including several sub-phenomena as combustion, spray evolution etc.), conduction in the solid and radiation. Each of them is solved in a dedicated simulation, running with a parallel coupling strategy. As in [22], instantaneous values are exchanged at the coupling iteration and consist of surface quantities for the solid-fluid and solid-radiation interactions, whereas volume quantities for the fluid-radiation coupling.

The procedure used in U-THERM3D is depicted in Figure 4. The CFD and conduction solvers advance in time with their own time-step. As far as radiation is concerned a steady solver is exploited because of the extremely small time scales. Convective and radiative wall heat fluxes are respectively converted in a Robin BC and black-body radiation BC before sending them to the conduction solver. On the other hand, wall temperature is used as Dirichlet BC by flow and radiative field computations,

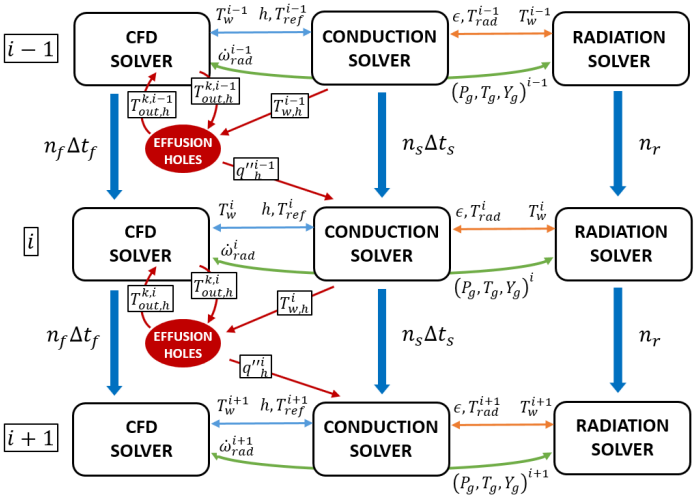

FIGURE 4. U-THERM3D parallel coupling strategy

then transferred to their respective solvers. Even though the employed mixed Dirichlet-Robin BC does not ensure a conservative behaviour at the interface, it provides a stable coupling. The inaccuracies, however, are definitely below the global error of the methodology if a high coupling frequency is set. Radiation solver requires some field variables from the CFD solver, that are gas pressure, temperature and composition. The resulting energy source due to absorption and emission phenomena is returned to the flow field computation.

User Defined Functions (UDFs) were written to handle the synchronisation of the solvers as well as, together with Scheme scripts, to exchange interface data.

As shown in Figure 4 a dedicated solver for the effusion holes is integrated into the procedure to compute heat sink effect. It relies on a 0-D computation of the energy balance within the hole and an imprinting technique to apply the fluid boundary conditions at the inlet/outlet of each hole. In the present work, this solver is not exploited as will be discussed in the next section. The interested reader is addressed to [24, 37] for details.

NUMERICAL SETUP

The present approach requires to set up three different simulations for the convective, conductive and radiative problems as shown in Figure 4. Pressure-velocity coupling was solved by the pressure-based SIMPLEC (Semi-Implicit Method for Pressure Linked Equations-Consistent) algorithm for the convective solver. Second order schemes were adopted to discretize both the advection and temporal terms.

Fluid time step was set to 3e-06 s according to the turbulence scales predicted on preliminary RANS simulations and keeping the CFL number close to 1 whereas the time scale of conduction

phenomenon was taken into account for the estimation of the solid time step that, therefore, was set to 1e-03 s. The coupling between the solvers occurred every 10 fluid time steps and 30 solid time steps.

The choice of computational domains as well as boundary conditions is depicted in Figure 5 and is, here, discussed.

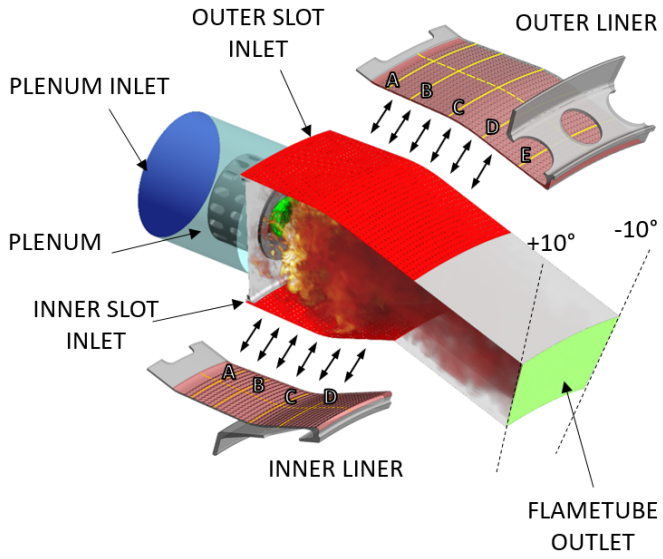

FIGURE 5. Computational domains and main boundary conditions.

Domains

The main benefits of an SRS are appreciated within the flametube because of the strong interaction between turbulence, combustion and spray evolution. Moreover, the focus of the present work is on the high-fidelity prediction of metal temperature, that is mostly affected by the unsteadiness on the hot side. Hence, in order to reduce computational time keeping a good accuracy, gas phase phenomena are solved in a domain including the flametube and an upstream plenum, unlike the RANS simulations in [24] where also the flow field on the cold side was simulated on a geometry representative of the real combustor. This simplification has even fewer effects on the radiative fluxes, that are negligible in the annulus if compared with the convective ones as reported on energy budgets in [24].

Solid conduction is computed in a physically-separated domain representing the inner and outer liners. Indeed, being the metal opaque for radiation, beams can be only absorbed or reflected at the fluid-solid interface.

Computational grids

The different requirements for the involved computations were taken into account during the mesh generation. As a result, three computational grids were created with ANSYS®Meshing. Mesh for the convective problem consists of nearly 8.7M tetrahedral elements. Making a mesh sensitivity to choose the proper space discretization in a multiphysics problem involving three grids is a time-consuming matter, so that the choice of mesh sizing was a compromise between computational cost and accuracy. As above mentioned, scale resolution in SAS has not an explicit dependency on grid spacing. However, its adequacy in the prediction of aerothermal field was widely evaluated in [25] where a grid sensitive study was carried out. As in the near-wall region the SAS model behaves as a RANS k-ω SST model, to exploit a wall function approach [27] the mesh counts 3 prismatic layers at wall and a y+ in the range of applicability for this wall treatment.

Radiation and solid meshes were recovered from [24]. In the former a drastic coarsening of the convective grid was performed to obtain a 4M tet-only elements mesh. Using a loose coupling for the fluid-radiation interaction together with a mesh coarsening can reduce the computational effort of the coupled problem of around $30-40\%$. The solid domain, instead, requires a huge refinement around the inner walls of the 2000 tiny effusion holes, resulting in 21.3M tetrahedral elements.

Boundary conditions

The boundary conditions were set according to [25] for the convection problem and to [24] for the remaining simulations. Concerning convective domain mass flow rate and static pressure were prescribed, respectively, at the inlet and outlet boundaries shown in Figure 5. Flow split was determined from preliminary RANS simulations with the multi-perforation modelled through point mass sources using the SAFE (Source based effusion model) methodology, presented in [38] and applied also in [39]. In the present work, effusion holes are grouped in rows where uniform boundary conditions are applied. Temperature at the plenum inlet, operating pressure and fuel mass flow rate were set according to the specific operating condition reported in Table 1. Boundary conditions for the radiation problem consist of absorbing/emitting walls, inlets and outlets. The hot sides of the two liners (red regions in Figure 5) were coupled with solid and, for this reason, coupling BCs are required. At the solid-fluid interfaces (i.e. in the conduction-convection and conduction-radiation couplings), convective and radiative heat fluxes are computed and converted in a Robin boundary condition and a black-body radiation (radiation temperature and emissivity), respectively. The obtained quantities are sent to the solid, which returns the wall temperature to the other simulations.

It is worth remember that the focus of the work is on the effects of a scale resolving modelling on the conjugate heat transfer problem and that such effects are either negligible as in the cold

side or computationally infeasible as within the effusion holes. As a result, heat transfer coefficients and reference temperatures were set on the above mentioned zones of the solid simulation, deduced from the results of THERM3D steady analysis on the full single sector geometry [24]. An analogous approach was adopted to impose the coolant temperature on the inlet patches representing the exit of the effusion holes. This assumption is justified by the small heat up of coolant crossing the multi-perforation. The remaining walls were treated as smooth, no slip and adiabatic.

Material properties

Solid was modelled as a metal alloy. Temperature-dependent properties were applied both to the metal and gas. For the latter, in addition, a dependency from progress variable and mixture fraction was set to include the effects of change in composition due to the combustion process. Properties taken from [34] were used to characterize Jet A-1 fuel. The spectral radiation is approximated with a weighted sum of gray gases, while metal emissivity is set 0.8.

RESULTS

In this section the results of the investigated test points will be presented, compared with the THERM3D results [24] and discussed. While the numerical setup of the different simulations was widely assessed in previous works [24, 25], the new tool (i.e. U-THERM3D) and the coupling settings required a preliminary validation. For this purpose, first of all, the Approach condition was simulated, analysed and compared with the experiments. Then, the present tool was applied to the Take-Off condition.

Approach

The aerothermal field is strongly influenced by the double swirler configuration and was widely discussed in [25] in the context of Scale-Resolving Simulations. The injection system creates a swirling flow with a large inner recirculation zone and two outer recirculation zones in the corners between dome and liners. A major part of liquid fuel is injected in the pressure atomizer (see Table 1), which breaks it up in droplets. These particles evaporate partially in the inner duct, contributing to feed the hot gases ingestion that periodically occurs within the swirler from the downstream recirculation zone. This behaviour can be observed in Figure 6 showing the temperature field in the combustor. While the timeframe chosen for the instantaneous temperature does not seem to be subject to flashback, the mean field highlights that gas at high temperature is present up to the pilot injector.

The core region of the flametube is unaffected by the coupled simulation at Approach if compared to the adiabatic simulation reported in [25]. The shear stresses and high velocities caused by the burner promotes the breakup of fuel film flowing on the airblast atomizer, the turbulence of jets and, as a results, the subsequent dispersion of the liquid particles as well as of the evaporated fuel. Large eddies trap the fuel into pockets where it is mixed and burnt, leading to hot spot regions moving downstream. These turbulent structures interact in a non-stationary fashion with the liners increasing convection and, therefore, wall heat transfer. Such a phenomenon was investigated in [24] on the adiabatic simulation, highlighting the differences between RANS and SAS in the prediction of the mean adiabatic wall temperature and the wide range of its fluctuations in the upstream region of the liner. Turbulent energy redistribution in the flametube has a key role in the heat transfer process as shown in the corner regions, where the mean temperature is definitely higher than the one obtained in [24]. This property is typical of SRSs that are able to solve a portion of turbulent diffusion.

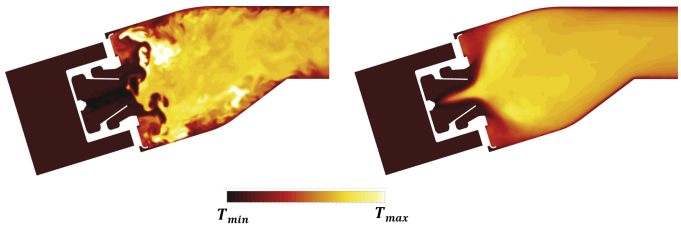

FIGURE 6. Contours of instantaneous (left) and mean (right) gas temperature at Approach condition.

In Figure 7 the instantaneous and mean energy source term due to radiation is shown, representing the data sent from the radiative to the convective simulation. Even if absorption and emission properties depend on species composition, the temperature is the main quantity affecting the energy source. The flame region has negative values and the higher the temperature, the more negative the energy sink. On the other hand, low temperatures in the mixing regions between film cooling and flue gases provide absorption of radiative energy.

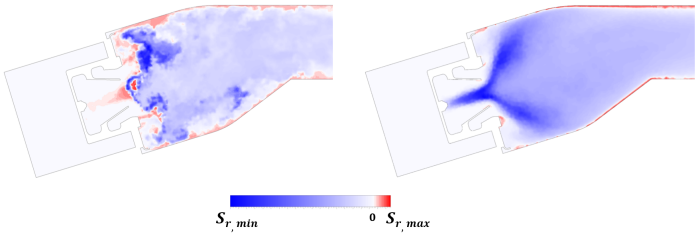

FIGURE 7. Contours of instantaneous (left) and mean (right) energy source term due to radiation at Approach condition.

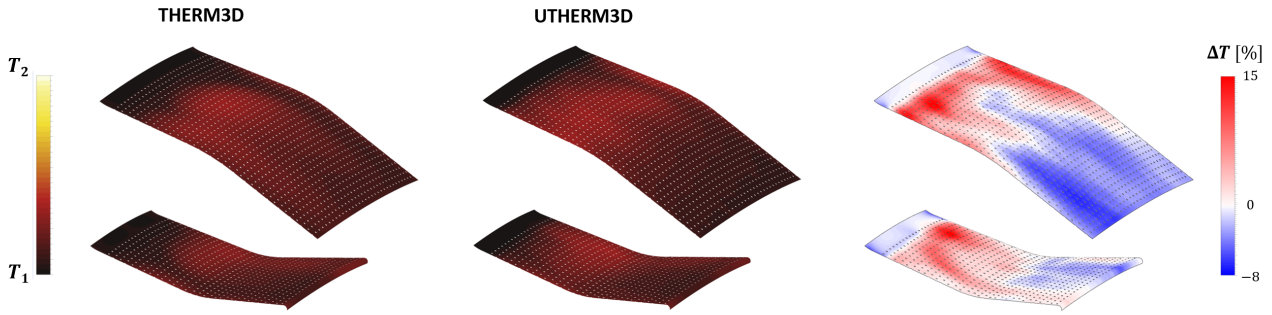

FIGURE 8. Contours of mean temperature on the hot side of the liners for the THERM3D (left) and U-THERM3D (middle) simulations at Approach condition. The relative difference between the latter and the former normalized by the THERM3D value (in [K]) is also reported (right).

Focusing on the two liners, the resolved part of turbulent convection affects the prediction of metal temperature if an unsteady coupling is exploited. Figure 8 shows the temperature distribution on the cold side of the liners for the THERM3D [24] and U-THERM3D simulations together with the relative difference (in percentage) between the latter and the former normalized by the THERM3D value (in [K]). If compared to the steady result, U-THERM3D predicts a broader high-temperature region and a smoother distribution. Indeed, the turbulent interaction between swirling flow and walls is detrimental for the film effectiveness of both the slot and effusion. Opposite cold streaks appeared on the two liners in the THERM3D modelling as the coolant was not disturbed by the swirling flow, maintaining a good protection. This feature disappears completely in the present simulation because of an increased jet opening angle of the swirling flow related to the unsteady treatment. As a result, in this region, temperature rises around 15% compared to a steady RANS coupling. Similar values are observed immediately downstream of the slot exit for the presence of hot gas recirculation in the corners. The liners show two different trends: the first half region is warmer but the downstream zone has lower temperatures.

A quantitative comparison with measurements of the liner temperature on the cold side reveals the improvements of the present multiphysics tool in the prediction of liner thermal load, as reported in Figure 9, 10 and 11 in terms of normalized temperature. The data were extracted on the lines highlighted in the sketch of Figure 5.

Figure 9 shows the temperature distribution of both the liners along the centerline, expressed as normalized curvilinear abscissa $\hat{s}$. The curves confirm the higher heat load of the U-THERM3D simulation at upstream locations already observed in Figure 8, especially for the Inner Liner. On this side, the numerical results are shifted towards measurements. The Outer Liner temperature, instead, was already well-predicted by THERM3D but the present approach, anyway, shows a further improved

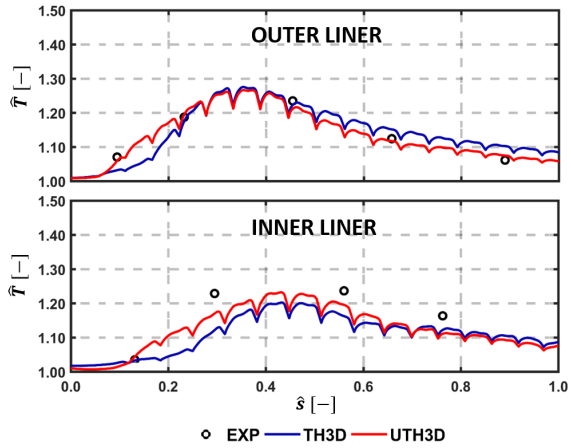

FIGURE 9. Comparison of the centerline temperature between experiments, THERM3D and U-THERM3D on the cold sides of the Inner Liner (top) and Outer Liner (bottom) at Approach condition.

trend. For instance, on the first measurement point a better agreement is obtained thanks to the smoothing effect of temperature gradients.

Analogous comparisons can be performed on the spanwise lines depicted in Figure 5 and the results are reported in Figure 10 for the Outer Liner (lines A,B,C,D,E) and in Figure 11 for the Inner Liner (lines A,B,C,D). Once again, U-THERM3D predicts smoother tangential distributions of metal temperature, in particular at B and C locations of the Inner Liner. While in RANS the swirling flow keeps a good film protection up to the fifth row of holes, in SAS computation the hot gases disrupt the coolant layer before the second row leading to a higher thermal load at line A that is confirmed by experiments. This interaction, however, is excessive at -10/10° locations on the Outer Liner resulting in an overestimated metal temperature. A general improvement in the distributions could be obtained revising the boundary conditions applied to the effusion holes. Indeed, a constant mass flow rate

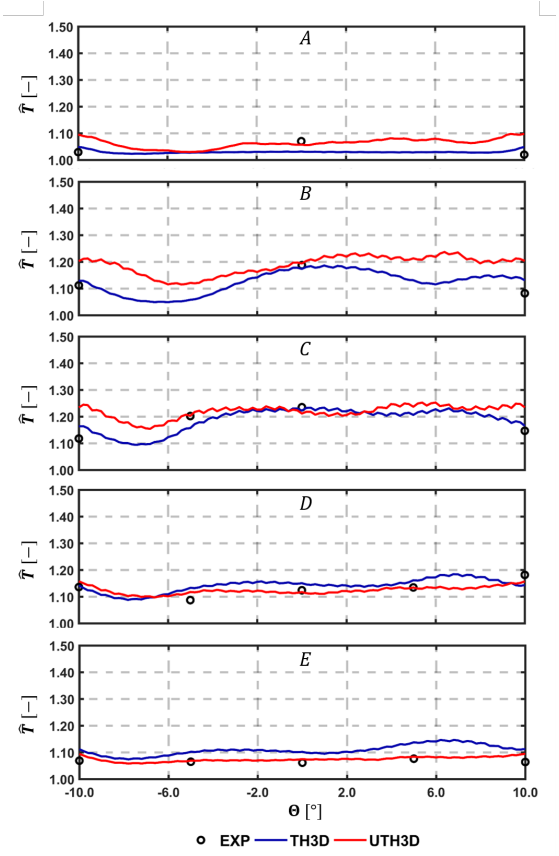

FIGURE 10. Comparison of the spanwise temperature between experiments, THERM3D and U-THERM3D on the cold sides of the Outer Liner for the locations depicted in Figure 5 at Approach condition.

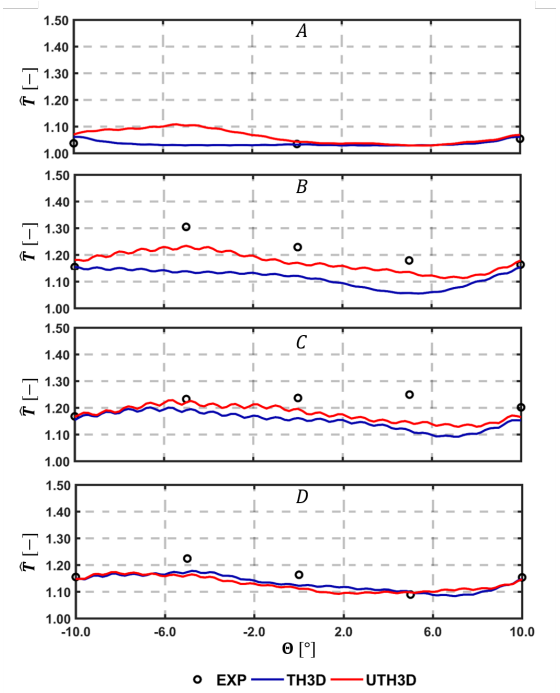

FIGURE 11. Comparison of the spanwise temperature between experiments, THERM3D and U-THERM3D on the cold sides of the Inner Liner for the locations depicted in Figure 5 at Approach condition.

was chosen for each row but the pressure distribution is not uniform in the tangential direction. This is particularly expected on the hot side because of the impinging of swirling flow on the liner walls that increases locally the pressure. This phenomenon is more relevant in the centerline region, resulting, in the hypothesis of uniform pressure on the cold side, in a decrease of pressure drop and, hence, in lower mass flow rate compared to the uniform injection. Obviously, more coolant will be injected from the holes close to -10/10° locations if the same total mass flow rate must be kept and the liner will be more protected in these regions. The solution-dependent distribution of coolant on both the tangential and axial directions are hardly predictable *a priori* and its effect on the heat load deserves further investigations in the future.

Take-Off

Increasing the power load by means *FAR*, *P*30 and *T*30 leads to higher burning rates, gas temperatures and ultimately more critical conditions for the liners. The hot core region moves up to the outlet, as noticeable in Figure 12. As at Approach, the

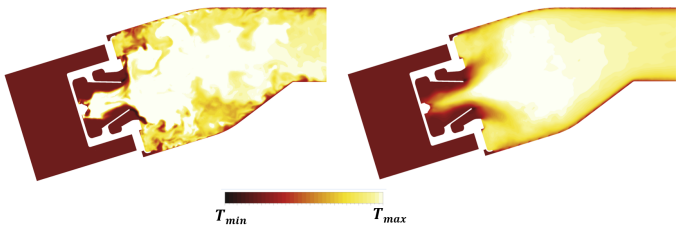

FIGURE 12. Contours of instantaneous (left) and mean (right) gas temperature at Take-Off condition.

flame propagates within the injector and can reach the proximity of the pilot atomizer. This phenomenon is visible in both the instantaneous and mean gas temperature, even if monitoring different time-steps have highlighted an alternating positioning of the flame in and out of the swirler. However, the mean opening angle of the swirling jet becomes more closed than at Approach because of the augmented flow rate.

The severe environment within the flametube causes a sig-

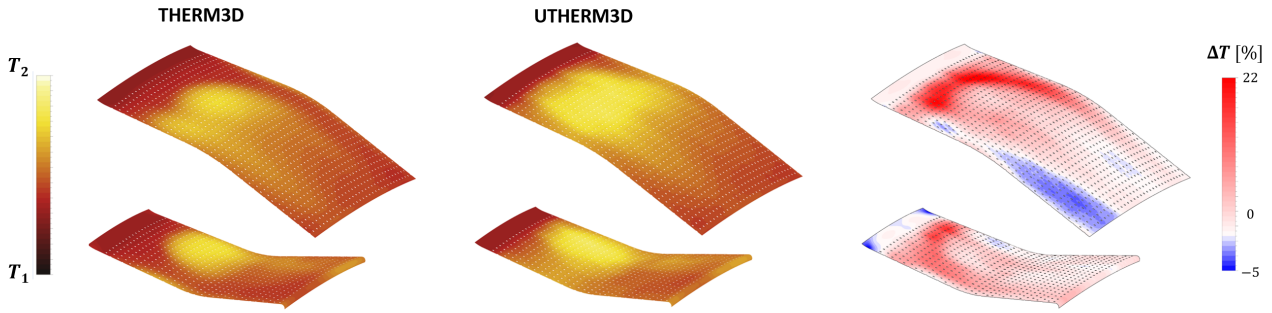

FIGURE 13. Contours of mean temperature on the hot side of the liners for the THERM3D (left) and U-THERM3D (middle) simulations at Take-Off condition. The relative difference between the latter and the former normalized by the THERM3D value (in [K]) is also reported (right).

nificant increase in the thermal stresses on the liner compared against the Approach condition, as illustrated by the metal temperature distribution reported in Figure 13. The wall temperature predicted by U-THERM3D is considerably higher than the values provided by the corresponding THERM3D simulation. Unlike the previous operating condition, a general increase of temperature is observed in almost all the surface with peak values of around 20% in a relative term, mainly located in the upstream region where the swirling flow interacts with the wall. In particular, as for Approach, the following considerations are still valid:

- The resolution of a portion of the turbulent convection spectrum smooths the temperature gradients;
- The resolved mixing increases the entrainment of hot gases in the outer recirculation zones resulting in an increase of metal temperature in the liner region closer to the slot exit;
- The swirling flow interacts with the slot and film cooling more uniformly in the spanwise direction, almost making the cold streaks of THERM3D disappear.

With a focus on the Outer Liner, the downstream half shows an opposite trend of the relative difference of temperature between an unsteady and steady simulation. Indeed, at the Approach condition, this region is warmed by gases having exchanged more heat with the primary zone of the liner and which, for this reason, are cooler. As the heat transfer in the primary zone is augmented in an unsteady way, the final region can be wet by colder gases resulting in a slightly lower metal temperature. On the other hand, at Take-Off hot radiating pockets are convected downstream to the mid-region of the liner, contributing to keep higher metal temperatures in the second half of the liner.

Similarly to Figure 9, Figure 14 shows again as using U-THERM3D the temperature rise is anticipated along the centerline axial direction, confirming the great impact on metal temperature of a scale-resolving prediction of the aerothermal field in the outer recirculation zone. The maximum value identifies jet-wall interaction phenomena, approximately located at 40% of the relative curvilinear abscissa for both the liners and the operating conditions. However, on the inner side, a second small peak region appears at 80% of the liner length that is also visible in the THERM3D simulation. This feature is caused by radiation, in terms of a greater weight of the shape factor on the thermal load for this operating point. The view factor from the flame and the dome to the second half of the Inner Liner is unfavourable because of the adopted combustor geometry, leading to a local peak in the radiative heat flux.

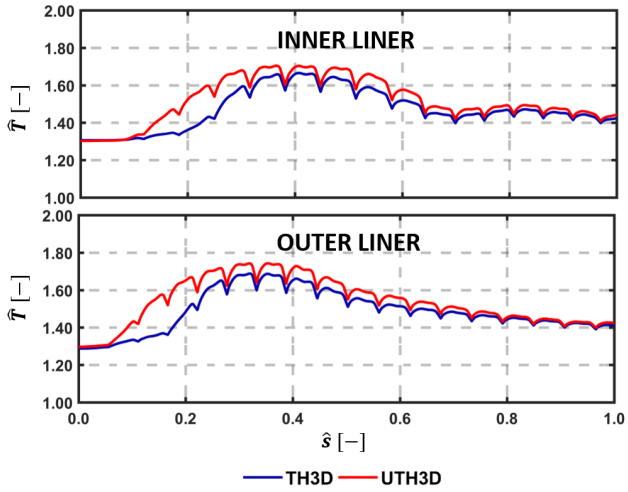

FIGURE 14. Comparison of the centerline temperature between experiments, THERM3D and U-THERM3D on the cold sides of the Inner Liner (top) and Outer Liner (bottom) at Take-Off condition.

Heat load analysis

A deep insight into the contribution of the different heat transfer modes to the thermal load can be useful to understand the metal temperature trends. For this purpose Figure 15 and Figure 16 show the energy budget for Inner Liner and Outer Liner, respectively. The total heat load normalized by a reference value

and divided into the convection (blue) and radiation (red) contributions is reported for the hot side (HS), cold side (CS) and effusion holes (EFF). The values are compared against the results obtained with THERM3D for both the operating conditions. The numbers above each bar highlight quantitatively the relative component of convection and radiation on the heating (HS) and cooling (CS+EFF) of the liner. The heat load follows the temperature trend, with a significant increase moving from Approach to Take-Off independently by the coupling strategy. However,

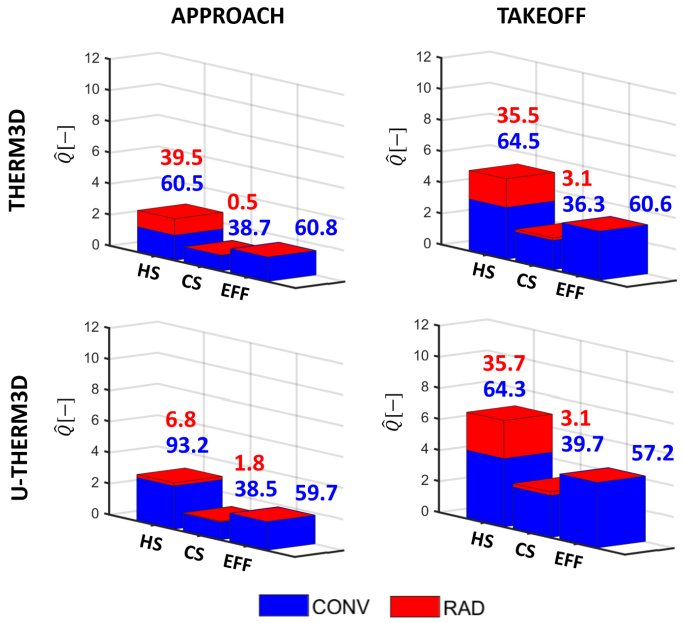

FIGURE 15. Comparison between THERM3D and U-THERM3D of the normalized total heat loads for the Inner Liner at Approach and Take-Off conditions. Values above the bars are the relative contribution of convection and radiation to the heating and cooling of the liner.

modelling conjugate heat transfer in an unsteady fashion in place of a steady framework modifies the relative weight of the heat transfer modes. At Approach, in the U-THERM3D simulation radiation it is reduced by the lower gas temperature. Moreover, the augmented convection caused by the prediction of higher heat transfer coefficients as well as a lower film protection increases the metal temperature making the contribution of radiation almost null. At Take-Off, instead, because of the widespread hot gas region provided by the SAS computation, the radiative heat load growths compared to both the Approach and the THERM3D results.

The heat load is more than doubled moving from Approach to Take-Off, closer to three times on the Outer Liner. The unbalanced distribution of radiative heat load between Inner and Outer

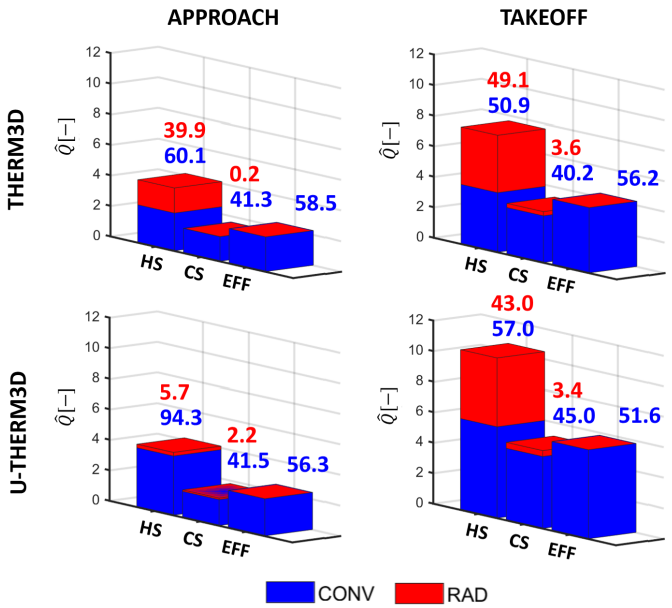

FIGURE 16. Comparison between THERM3D and U-THERM3D of the normalized total heat loads for the Outer Liner at Approach and Take-Off conditions. Values above the bars are the relative contribution of convection and radiation to the heating and cooling of the liner.

liners can be attributed to the annular geometry of the combustor, which makes high view factors from the Inner Liner and the flame to the Outer Liner. On the other hand, the Outer Liner views the Inner Liner with a lower factor. As a result, the latter radiates completely to the former which, however, radiates partially itself. Inhomogeneities in the wall to wall radiation become more relevant when metal temperature is higher, as at Take-Off. This result is also confirmed by the relative contribution of convection and radiation that is around 65%/35% for the Inner Liner and 55%/45% for the Outer Liner.

As evident in Figure 15 and Figure 16 the cooling function is largely demanded to the effusion system, whose weight on liner cooling is 56% on average. The absolute value is almost unchanged at Approach using the present unsteady coupling procedure but the increase is evident at Take-Off as a result of the higher metal temperature predicted by U-THERM3D.

CONCLUSIONS

Conjugate heat transfer is a challenging problem that in gas turbine combustors is made even more complex by multiphysics interactions. A deep insight of the involved phenomena cannot be obtained with experimental campaigns on real aeroengine burners. The increasingly widespread exploitation of massively parallel computing is pushing CFD as a tool supporting the final design of modern combustors, which is characterized by several

strict constraints. Among all design requirements, the control on metal temperature is one of the most pursued.

This paper illustrates the main findings of numerical investigations aimed at providing a better understanding of the thermal load on an aeronautical effusion-cooled lean burn combustor. A desynchronized loose coupling methodology, called U-THERM3D, was proposed to simulate the whole time-consuming multiphysics problem and applied in the framework of a full-annular test carried out in a EU-funded research program. Several aspects of the numerical modelling were already assessed on the same burner during previous works, in steady [24] and unsteady [25] context. Two different conditions were simulated, representative of the Approach and Take-Off operations of an aeroengine. The results of the present methodology were compared with the steady multiphysics tool THERM3D obtained in [24] and with measurements as far as the Approach is concerned.

Simulations were run for roughly 45000 CPU hours, a computational time one order of magnitude greater than the one required by the equivalent steady coupling. Despite the computational cost, the new tool provides a general increase of metal temperature and a smoother distribution that improve the prediction of liner temperature, as confirmed by a comparison with the experimental data. A common feature in the two test points is the strong increase of temperature in the first half of the liner related to the resolution in SAS framework of the turbulent interaction between the swirling flow and the walls. Indeed, the Scale-Resolving Simulation is able to predict the hot gases entrainment in the outer recirculation zones, the local growth of heat transfer coefficient and the unsteady sweeping of film cooling. While convection increases, a heat load analysis reveals opposite trends for radiation in the two operating conditions moving from a steady to an unsteady coupling. At Approach, maximum gas temperature does not change compared to THERM3D simulation and, together with the higher wall temperature, eliminate the contribution of radiation. On the other hand at Take-Off the heat transferred by radiation rises slightly because of the widespread hot gases volume within the flametube. Similarly to the THERM3D solution, the ratio between convection and radiation is around 65%/35% and 55%/45% for the Inner and Outer liners, respectively. Here, the major weight of radiation in the Outer Liner can be explained by the annular geometry of the combustor that provides self-viewing properties to the outer concave surface. Hence, the present work highlights that a proper modelling of the aerothermal field with Scale-Resolving Simulations can be effective in the prediction of liner temperature and can reveal unexpected changes in the relative contribution of heat transfer modes compared to a steady modelling. The acceptable prediction of metal temperature obtained by U-THERM3D shows the potential of this tool as a framework for the high-fidelity thermal design of gas turbine combustors. Obviously, the accuracy of the coupled simulation can benefit from the improvement of the different involved models and to the authors' opinion research effort should be focused on this task.

ACKNOWLEDGMENT

This activity was performed in the context of the EU-funded research programme LEMCOTEC (Low Emissions Core-Engine Technologies), a Collaborative Project co-funded by the European Commission within the Seventh Framework Programme (2007-2013) under the Grant Agreement n° 283216.

The authors wish to gratefully acknowledge GE Avio S.r.l. for providing us the results of the experimental campaign carried out at CIAM.

References

[1] ICAO. Aviation benefits. Report, International Civil Aviation Organization, 2017.

[2] Moreno, V. Combustor liner durability analysis. 1981.

[3] McGuirk, JJ. The aerodynamic challenges of aeroengine gas-turbine combustion systems. *The Aeronautical Journal*, 118(1204):557–599, 2014.

[4] Wadia, A. R. Advanced Combustor Liner Cooling Technology for Gas Turbines. *Defence Science Journal*, 38(4): 363–380, January 2014.

[5] Gustafsson, K. M. B. and Johansson, T. G. An Experimental Study of Surface Temperature Distribution on Effusion-Cooled Plates. *ASME J Gas Turb Pwr*, 123(2): 308–316, January 2001. ISSN 0742-4795. doi: 10.1115/1.1364496.

[6] Andrews, G. E., Asere, A. A., Gupta, M. L., and Mkpadi, M. C. Full Coverage Discrete Hole Film Cooling: The Influence of Hole Size. page V003T09A003, March 1985. doi: 10.1115/85-GT-47.

[7] Martiny, M., Schulz, A., and Wittig, S. Full coverage film cooling investigations adiabatic wall. In *International congress, Gas turbine and aeroengine*, 1995.

[8] Florenciano, J. L. and Bruel, P. LES fluid-solid coupled calculations for the assessment of heat transfer coefficient correlations over multi-perforated walls. *Aerospace Science and Technology*, 53:61–73, June 2016. doi: 10.1016/j.ast.2016.03.004.

[9] Wurm, B., Schulz, A., Bauer, H.-J., and Gerendas, M. Impact of Swirl Flow on the Cooling Performance of an Effusion Cooled Combustor Liner. *ASME J Gas Turb Pwr*, (134):121503–1:121503–9, 2012.

[10] Wurm, B., Schulz, A., Bauer, H.-J., and Gerendas, M. Cooling efficiency for assessing the cooling performance of an effusion cooled combustor liner. *Proceedings of ASME Turbo Expo*, (GT2013-94304), 2013.

[11] Wurm, B., Schulz, A., Bauer, H.-J., and Gerendas, M. Impact of swirl flow on the penetration behaviour and cooling

performance of a starter cooling film in modern lean operating combustion chambers. *Proceedings of ASME Turbo Expo*, (GT2014-25520), 2014.

[12] Andreini, A, Caciolli, G, Facchini, B, Picchi, A, and Turrini, F. Experimental investigation of the flow field and the heat transfer on a scaled cooled combustor liner with realistic swirling flow generated by a lean-burn injection system. *ASME J Turbomac*, 137(3):031012, 2015.

[13] Andreini, A, Becchi, R, Facchini, B, Mazzei, L, Picchi, A, and Turrini, F. Adiabatic effectiveness and flow field measurements in a realistic effusion cooled lean burn combustor. *ASME J Eng Gas Turb Pwr*, 138(3):031506, 2016.

[14] Andreini, A, Facchini, B, Becchi, R, Picchi, A, and Turrini, F. Effect of slot injection and effusion array on the liner heat transfer coefficient of a scaled lean-burn combustor with representative swirling flow. *ASME J Eng Gas Turb Pwr*, 138(4):041501, 2016.

[15] Andreini, A., Becchi, R., Facchini, B., Picchi, A., and Peschiulli, A. The effect of effusion holes inclination angle on the adiabatic film cooling effectiveness in a three-sector gas turbine combustor rig with a realistic swirling flow. *International Journal of Thermal Sciences*, 121:75–88, 2017.

[16] Andreini, A, Bertini, D, Facchini, B, and Puggelli, S. Large-eddy simulation of a turbulent spray flame using the flamelet generated manifold approach. *Energy Procedia*, 82:395–401, 2015.

[17] Puggelli, S., Bertini, D., Mazzei, L., and Andreini, A. Assessment of scale-resolved computational fluid dynamics methods for the investigation of lean burn spray flames. *ASME J Eng Gas Turb Pwr*, 139(2):021501, 2017.

[18] Puggelli, S, Bertini, D, Mazzei, L, and Andreini, A. Modeling strategies for large eddy simulation of lean burn spray flames. *ASME J Gas Turb Pwr*, 140(5):051501, 2018.

[19] Fadl, M and He, L. On LES based conjugate heat transfer procedure for transient natural convection. In *ASME Turbo Expo 2017: Turbomachinery Technical Conference and Exposition*, pages V05AT10A002–V05AT10A002. American Society of Mechanical Engineers, 2017.

[20] He, L and Fadl, M. Multi-scale time integration for transient conjugate heat transfer. *International Journal for Numerical Methods in Fluids*, 83(12):887–904, 2017.

[21] Berger, Sandrine, Richard, Stéphane, Staffelbach, Gabriel, Duchaine, Florent, and Gicquel, Laurent. Aerothermal prediction of an aeronautical combustion chamber based on the coupling of large eddy simulation, solid conduction and radiation solvers. In *ASME Turbo Expo 2015: Turbine Technical Conference and Exposition*, pages V05AT10A007–V05AT10A007. American Society of Mechanical Engineers, 2015.

[22] Jaure, S., Duchaine, F., Staffelbach, G., and Gicquel, L. Y. M. Massively parallel conjugate heat transfer methods relying on large eddy simulation applied to an aeronautical combustor. *Computational Science & Discovery*, 6(1): 015008, 2013. doi: 10.1088/1749-4699/6/1/015008.

[23] Koren, C., Vicquelin, R., and Gicquel, O. Self-adaptive coupling frequency for unsteady coupled conjugate heat transfer simulations. *International Journal of Thermal Sciences*, 118:340–354, August 2017. doi: 10.1016/j.ijthermalsci.2017.04.023.

[24] Bertini, D., Mazzei, L., Puggelli, S., Andreini, A., Facchini, B., Bellocci, L., and Santoriello, A. Numerical and experimental investigation on an effusion-cooled lean burn aeronautical combustor: aerothermal field and metal temperature. In *Proceedings of ASME Turbo Expo*, 2018.

[25] Mazzei, L., Puggelli, S., Bertini, D., Andreini, A., Facchini, B., Vitale, I., and Santoriello, A. Numerical and experimental investigation on an effusion-cooled lean burn aeronautical combustor: Aerothermal field and emissions. *ASME J Gas Turb Pwr*.

[26] Egorov, Y. and Menter, F. R. Development and application of SST-SAS turbulence model in the DESIDER Project. *Second Symposium on Hybrid RANS-LES Methods*, 2007.

[27] ANSYS. *ANSYS Fluent, 17.1 Theory Guide*, January 2016. Canonsburg, PA, USA.

[28] Donini, A., Bastiaans, R. J. M., Van Oijen, J. A., and de Goey, L. P. H. The Implementation of Five-Dimensional FGM Combustion Model for the Simulation of a Gas Turbine Model Combustor. *ASME J Gas Turb Pwr*, June 2015.

[29] Sirjean, B., Dames, E., Sheen, D. A., Wang, H., Lu, T. F., and Law, T. F. Jetsurf 1.0-ls: Simplified chemical kinetic models for high-temperature oxidation of C5 to C12 n-Alkanes. Technical report, http://melchior.usc.edu/JetSurF1.0/JetSurF1.0-ls, 2009.

[30] Morsi, S. A. and Alexander, A. J. An Investigation of Particle Trajectories in Two-Phase Flow Systems. *Journal of Fluid Mechanics*, 55:193–208, 1972.

[31] Reitz, R.D. Modeling atomization processes in high-pressure vaporizing sprays. *Atomisation Spray Technology*, 3:309–337, 1987.

[32] Abramzon, B. and Sirignano, W. A. Droplet vaporization model for spray combustion calculations. *International journal of heat and mass transfer*, 32(9):1605–1618, 1989.

[33] Ranz, W. E. and Marshall, W. R. Jr. Vaporation from drops, part i. *Chem. Eng. Prog.*, 48(3):141–146, 1952.

[34] Rachner, M. Die Stoffeigenschaften von Kerosin Jet A-1. Technical report, DLR, Institut für Antriebstechnik, März 1998.

[35] Murthy, JY and Mathur, SR. Finite volume method for radiative heat transfer using unstructured meshes. *Journal of thermophysics and heat transfer*, 12(3):313–321, 1998.

[36] Mazzei, Lorenzo, Puggelli, Stefano, Bertini, Davide, Pampaloni, Daniele, and Andreini, Antonio. Modelling soot production and thermal radiation for turbulent diffusion

flames. *Energy Procedia*, 126:826–833, 2017.

[37] Mazzei, L. A 3d coupled approach for the thermal design of aero-engine combustor liners. *PhD Thesis - Universitá degli Studi di Firenze*, 2014.

[38] Andreini, A., Da Soghe, R., Facchini, B., Mazzei, L., Colantuoni, S., and Turrini, F. Local source based cfd modeling of effusion cooling holes: Validation and application to an actual combustor test case. *ASME J Gas Turb Pwr*, 136(1):011506, 2014.

[39] Mazzei, L, Andreini, A, Facchini, B, and Bellocci, L. A 3d coupled approach for the thermal design of aero-engine combustor liners. *Proceedings of ASME Turbo Expo*, (GT2016-56605), 2016.